3 Advances in Three-Dimensional Metal Oxide-Based Nanostructures for Biological Gas-Sensing Applications

Tushar Kanta Sahu

Abstract

Nanostructured materials have been widely studied and established for various sensing applications in the last few decades. Nevertheless, there are still outstanding problems that need to be dissected to further boost their performance, reliability, and cost-effectiveness. Herein, three-dimensional (3D) metal oxide-based nanostructured materials and their implementation in various sensing devices are discussed. Furthermore, the significance of apprehension and modulating the 3D design frameworks is explored to achieve more effective sensing devices for different healthcare issues.

Keywords

Breath biomarkers · Volatile organic compounds · Disease diagnosis · Metal oxide-based semiconductors · Environmental sensing · Food quality and safety

3.1 Introduction

Metal oxide-based semiconductors (MOSs) are known for their tunable morphological, optical, and electrical properties and, hence, most popular for gas-sensing applications. Among various MOSs, n-type metal oxides such as WO_3, In_2O_3, ZnO, Fe_2O_3, and SnO_2 are known for their promising performances in various gas-sensing applications (Yuan et al. 2019; Ren et al. 2020; Li et al. 2021; Ma et al. 2020; Zhao et al. 2020; Zhou and Zhang 2021). The gas-sensing applications of p-type metal oxides are relatively limited due to their low sensitivity as compared to

T. K. Sahu (✉)
Department of Materials and Environmental Chemistry, Stockholm University, Stockholm, Sweden
e-mail: tusharkanta.sahu@mmk.su.se

B. Purohit, P. Chandra (eds.), *Surface Engineering and Functional Nanomaterials for Point-of-Care Analytical Devices*, https://doi.org/10.1007/978-981-99-3025-8_3

n-type metal oxides. Design and construction of nanomaterials with special morphology and nanostructure has a crucial role in enhancing the selectivity and limit of detection (LoD) (Zhou and Zhang 2021). Generally, three-dimensional (3D) nanostructures with variable geometry and crystal facets provide higher surface area and a greater number of active sites which results in efficient gas-sensing applications (Zhou and Zhang 2021). In this chapter, we will briefly discuss about the recent advances in 3D nanostructure-based materials for biological gas-sensing applications.

3.1.1 Principles of Gas Sensing

The general functioning principles of a MOSs-constructed device for gas-sensing detection comprise the variations of electrical properties. So, when a specific gas comes in contact with the sensor, it will change the resistance of materials which is sensitive to gases (Neri 2015; Zhang et al. 2020). If the chemical adsorption of the gas molecules on the semiconductor surface is strong enough, then they exchange electrons between them. This directed to an alteration in the concentrations of charge carriers and as a result conductivity of the materials also changes (Fig. 3.1a) (Neri 2015). The amount of gas adsorbed directly depends on the concentration of the target gas, which in terms set the affiliation between the resistance value and concentration of target gas.

The mechanistic path involving n-type MOSs is shown in Fig. 3.1b (Kim and Lee 2014; Gurlo et al. 2005). In this type of sensing device, the oxygen molecules from air are adsorbed on the surface and interact with the electrons of sensing materials. These adsorbed oxygen molecules ionize to O_2^-, O^-, and O^{2-} depending on the working temperature. These working temperatures are generally high for MOSs-based sensing devices (Zhou and Zhang 2021). The interlinkage within the sensing surface and target gas results in the formation of a depletion layer, which further consequences in the increase of resistance due to an increase in potential barriers. Based on these mechanisms, reducing gases such as CO, H_2, acetone, ethanol, etc.

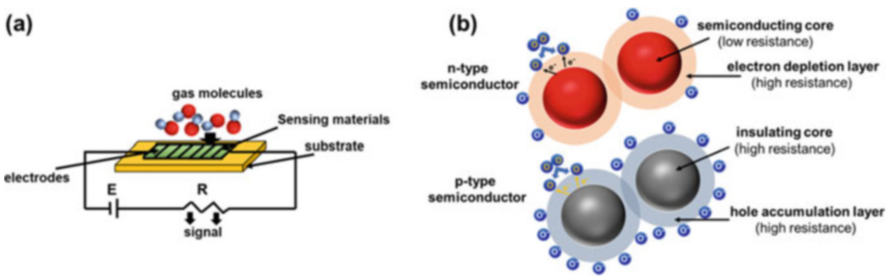

Fig. 3.1 (**a**) Detection circuit of a MOSs-based sensor [Reproduced with permission from Ref. (Zhang et al. 2020), copyright Elsevier] and (**b**) working mechanism for MOSs-based sensors. [Reproduced with permission from Ref. (Kim and Lee 2014), copyright Elsevier]

reduces the resistance, whereas oxidizing gases such as SO_2, NO_X, O_3, etc. increase the resistance (Zhang et al. 2020).

Besides MOSs, for other gas-sensing materials based on carbon and MXene, the oxygen molecules adsorption is not necessary for sensing. Herein, the mechanism involves physisorption of target gases on the surface of sensing devices, and they interact through van der Walls or the donor-acceptor interaction. Presence of various functional groups such as -OH, $-$COOH, and $=$ O also increases the gas molecules adsorption. Also, the number of adsorption sites on the sensing material surfaces and higher binding energy between target gases and sensing surfaces gives rise to efficient detection of gas molecules (Zhou and Zhang 2021; Degler et al. 2019).

3.2 Analytical Performance of Gas Sensors

The performance of sensor devices can be identified by numerous constraints which include the limit of detection, selectivity, sensitivity, cross-sensitivity, response and recovery times, stability, and lifetime. Based on these constraints, the functioning qualities of gas-sensing devices are quantified.

The lowermost concentration of the gas analyte that can be measured by the sensing devices is termed as the limit of detection (LoD). The LoD is a central constraint to know the aptness of any type of gas sensor. For example, when gas sensors are premeditated for air quality nursing, based on their LoD values, it can be checked if they are suitable for the sensing or not. Table 3.1 shows the threshold boundaries of the key air pollutants set by the National Ambient Air Quality Standards (NAAQS) in the USA and also by the European Union (EU) in Europe (Isaac et al. 2022). Although Table 3.1 only shows the LoD values, it is necessary to consider other parameters such as selectivity, cost-effectiveness, and robustness before employing the sensors for air quality nursing.

Table 3.1 European Union and US agencies approved threshold limits for some common pollutants with LoD of best-performing sensors reported in the literature

Pollutant	Threshold limits as per EU	Threshold limits as per the USA	Best-performing sensor (in terms of LoD)	References
CO	10 ppm	9 ppm	1 ppm	Lin et al. (2018)
CO_2	N/A	N/A	150 ppb	Willa et al. (2015)
SO_2	130 ppb	75 ppb	38 ppb	Prajapati and Bhat (2018)
O_3	120 ppb	70 ppb	20 ppb	da Silva et al. (2017)
NO_2	50 ppb	53 ppb	5 ppb	Rossinyol et al. (2007)

The sensitivity of a sensing device can be demarcated as the alteration in electrical signal with respect to the concentration of the target gas. It is represented as the ratio between the response signal when the sensing device is exposed to the target gas analyte and the response signal in the presence of air:

$$S = \frac{R_g}{R_a} \tag{3.1}$$

where R_g represents the resistance of air containing a fixed concentration of target gas and R_a represents the resistance in pure air. The sensitivity of a sensing device is dependent on external factors such as humidity and operating temperature and also on the intrinsic properties of the sensing materials (Wang et al. 2010).

The dynamic behavior of a gas sensor can be expressed by its response and recovery times. The definition of response time is the time required to attain a stable signal by the sensing devices when exposed to a specific amount of target gas, whereas the recovery time is the time required for a sensing device to reappearance to its original value in the absence of target gas. Typically, the response time is calculated when the signal takes 90% of the saturation signal and the response time is 10% of the saturation signal. This is for the reason that vast majority of the sensing devices take quite a few hours to reach the concluding saturation value due to slower kinetics after certain time (Isaac et al. 2022).

The aptitude of a gas sensor to identify a target gas among other various gases is titled its selectivity. It is a crucial parameter because numerous gaseous species present with the target gas can change the resistance with a similar way as of the target gas (Seinfeld and Pandis 1998). The reproducibility or stability of a gas sensor is also important for real-world applications as it reflects the ability of the sensing devices to reproduce the same signal when exposed to the target gas several times (Bochenkov and Sergeev 2010).

3.3 3D Nanostructures for Gas Sensing

Although many low-dimensional sensing devices including nanostructures of 0D, 1D, and 2D have been utilized in gas sensing, the main issues which hinder the functioning of these gas-sensing devices are structural stability, dispersibility, and sensibility. However, 3D nanostructures developed by incorporation of low-dimensional particles can overcome the abovementioned drawbacks with excellent gas-sensing applications.

3.3.1 3D Gas Sensors for Environmental Applications

Pollution of air by pollutant gas such as CO, CO_2, SO_2, NO_x, CH_4, etc. is a serious global concern as it is harmful to the environment as well as humans due to hasty industrialization, usage of agrochemicals, and the incineration of fuels. Besides this,

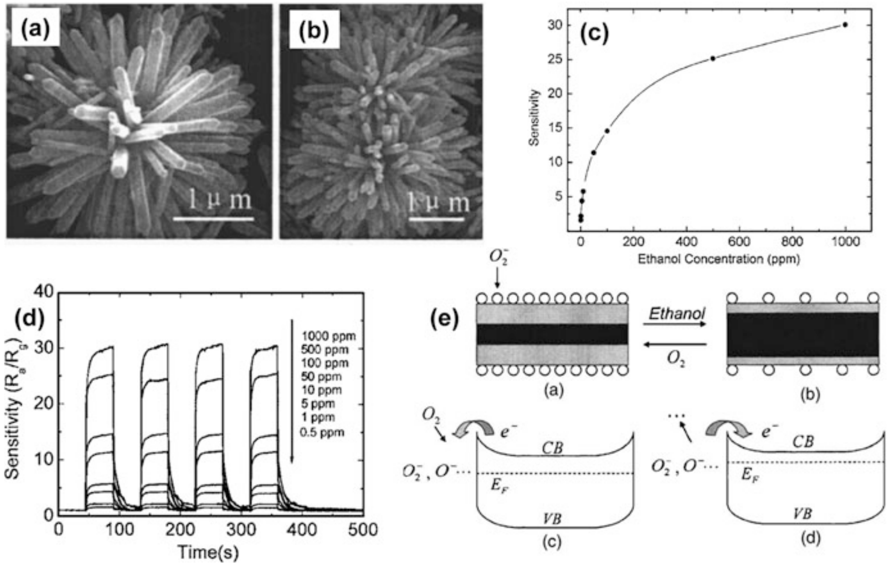

Fig. 3.2 (**a**, **b**) SEM images of flowerlike ZnO nanostructures composed of nanorods, (**c**) the sensitivity of sensors vs ethanol concentration, (**d**) the sensitivity response of sensors vs ethanol concentration, and (**e**) the mechanism involving the sensing of ethanol. [Reprinted with permission from Ref. (Feng et al. 2005), copyright AIP Publishing]

other gaseous pollutants such as NH_3, benzene series, CH_2O, etc. originating from industries also severely affect the human health when the exposed limit is exceeded (Mirzaei et al. 2016). Therefore, it is essential to oversee the concentration of these harmful gases for better environment.

3D nanostructures create a better ohmic contact with the substrate it is grown as compared to 1D nanostructures. For example, it was found that 3D hierarchical superstructure of ZnO grown over an FTO substrate has a lower ohmic resistance as compared to 1D ZnO nanowires as reported by Ansari et al. (Ansari et al. 2018). Besides, 3D hierarchical superstructure of ZnO with a large surface area and higher electron mobility results in better NH_3 sensing as compared to 1D nanowires of ZnO. Besides morphology, the defects and porosity existing in the 3D ZnO mesoporous thin films are also beneficial for sensing of NO_2 gas (Patil et al. 2018; Mane et al. 2021). Also, the 3D morphology of ZnO gives rise to porous structure and high surface area as compared to lower-dimensional ZnO nanostructures which facilitate better transport of mass and diffusion of gas in the sensing material (Mane et al. 2021). Krishnakumar et al. premeditated the effect of various 3D nanostructures of ZnO (flowerlike, starlike, spherical) for sensing of CO gas. All these nanostructures were prepared by a microwave-assisted method. It was found that the nanostructure with flowerlike morphology is more efficient for CO gas sensing than the other two nanostructures due to its trivial crystallite size, larger surface area, and modified barrier in potential (Krishnakumar et al. 2009; Feng et al. 2005). Figure 3.2 shows the sensitivity of ethanol sensing with 3D flowerlike nanostructures of ZnO. SnO_2 nanostructures also have potential applications as gas sensors due to its upright selectivity as well as sensitivity to various gases. SnO2 with different morphologies have been extensively explored for gas sensing (Firooz et al. 2009; Periyasamy and Kar 2020; Wang et al. 2016; Yuliarto et al. 2015). Also, 3D nanostructures of WO_3 are efficient in sensing NO_2 gas with superior selectivity (Cao et al. 2020).

Although, many gas sensors reported in the literature are effective in terms of lower value of LoD and good selectivity, however, operating temperatures for these sensors are very high. For actual environmental applications, gas sensors with lower operating temperature are needed to construct a long-term stable monitoring device.

3.3.2 3D Gas Sensors for Breath Analysis

Exhaled breath samples of human are very complex as it consists of carbon dioxide, nitrogen, oxygen, nitric oxide, and thousands of volatile organic compounds (VOCs). Among them, many VOCs have clinical significance as a biomarker for identification of some specific diseases (Alam et al. 2019). For example, a high level of acetone, nitric oxide, ammonia, hydrogen sulfide, and toluene are typically associated with diabetes, asthma, renal disease, halitosis, and lung cancer, respectively (Awano et al. 2008; Shin et al. 2012; Narasimhan et al. 2001; Gouma and Kalyanasundaram 2008; Peng et al. 2009; Yoon and Lee 2017). Table 3.2 shows some exhaled breath biomarkers related to diseases with their permissible limit (Das and Pal 2020). So, analyzing human respired breath samples through gas sensing characterizes a simple, economical, and faster method for disease diagnosis and prevention. However, the concentrations of disease-associated biomarker are very little (in ppb level). Therefore, gas sensor used for this type of operation should be highly selective toward a specific VOC with very low LoD (Konvalina and Haick 2014).

Table 3.2 Exhaled breath biomarkers related to diseases and their permissible limit

Biomarker	Related diseases	Maximum permissible limit
Acetone	Diabetes	0.9 ppm
NO	Asthma, lung cancer	25 ppb
H_2S	Ischemia, asthma, Down syndrome, Alzheimer's disease, halitosis, etc.	8–16 ppb
NH_3	Cirrhosis of the liver, halitosis, peptic ulcer, liver dysfunction, renal failure, etc.	250 ppb
Methane	Liver diseases, breast cancer, colon- and intestine-related diseases, asthma, etc.	–
Aldehydes	Alzheimer's disease; cancers, viz., lung cancer, breast cancer; Parkinson's disease; Wernicke's encephalopathy; etc.	–
Isoprene	Diabetes, hypercholesterolemia	105 ppb

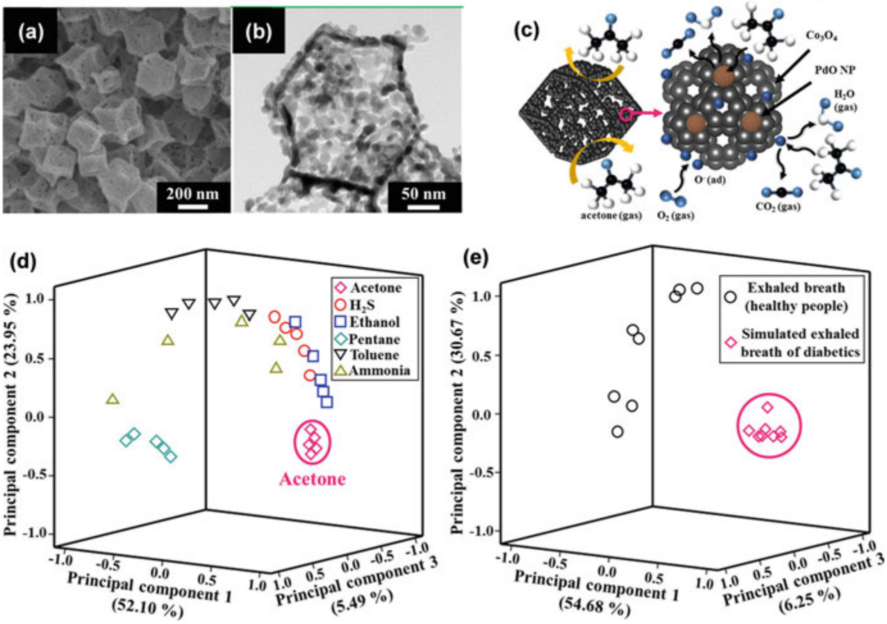

Fig. 3.3 (**a**) SEM image of PdO nanoparticle-functionalized Co_3O_4 hollow nanocages, (**b**) TEM image of PdO nanoparticle-functionalized Co_3O_4 hollow nanocage, (**c**) schematic illustration of acetone-sensing mechanism for PdO nanoparticle-functionalized Co_3O_4 hollow nanocage, (**d**) acetone sensing in presence of various interfering gases, and (**e**) acetone sensing of exhaled breath. [Reprinted with permission from Ref. (Konvalina and Haick 2014), copyright American Chemical Society]

Using metal-organic framework (MOF) templates, Koo et al. synthesized PdO nanoparticle-functionalized Co3O4 hollow nanocages (Koo et al. 2017). The morphological features are shown in Fig. 3.3a and b. The mechanism involving acetone sensing is shown in Fig. 3.3c. In this study, acetone sensing was demonstrated to be highly selective against other interfering gases by using hollow Co_3O_4 nanocages with high surface area and higher catalytic activity (Fig. 3.3d). Moreover, as shown in Fig. 3.3e, the sensor was also capable of distinguishing diabetic exhaled breath from that of normal people. Similarly, PdO-loaded $NiO/NiCo_2O_4$ truncated nanocages, SnO_2 multichannel nanofibers loaded with PtO_2 catalysts, and 3D inverse opal In_2O_3 microspheres show excellent acetone-sensing capabilities due to larger specific surface area, size-tunable pores, periodic porous structure, and highly 3D interconnection (Chen et al. 2018; Jeong et al. 2018; Wang et al. 2018).

The abnormal concentration of hydrogen sulfide (H_2S) in exhaled breath is a biomarker for diseases such as ischemia, asthma, Down syndrome, Alzheimer's disease, and halitosis (Jha et al. 2008; Huber et al. 2017; Kamoun et al. 2003; McGeer and McGeer 2010; Choi et al. 2014). For selective H_2S sensing, Yang et al. designed and fabricated inverse opal 3D WO_3 structures modified with ZnO@Au nanoparticles derived from MOF (Yang et al. 2020). The detection limit was 50 ppb at 170 °C and attributed to increased adsorption energies, a higher negative charge of O, and improved conductivity. Similarly, ZnO encapsulated in MOFs containing Pt nanoparticles showed good H_2S-sensing response (Zhou et al. 2022). Smaller Pt nanoparticles present in the MOF cavities activated the H2S sensing. The molecular-sieving effect of MOF (ZIF-8) resulted in high selectivity. It was also found that MOF-derived metal oxides are effective in gas sensing because of their high surface area (Wang et al. 2021; Shi et al. 2022; Wu et al. 2022).

3.3.3 3D Gas Sensors for Food Quality and Safety

Thousands of people are affected by food poisoning every year by consuming food contaminated by parasites, bacteria, and viruses. Early recognition of spoiled food can prevent many serious health issues. The spoiled food which creates poison and the vapors released from this poison can be distinguished using gas sensors (McCabe-Sellers and Beattie 2004).

Many kinds of seafood including fish, due to biodegradation during spoilage, release gases like dimethylamine (DMA) and trimethylamine (TMA) (Messenger et al. 2013). These gases can be used a marker for determining the freshness of this kind of foods. As reported by Sui et al., 3D α-MoO_3 flowers with hierarchical structure can effectively detect TMA among various other VOCs with LoD as low as 0.5 ppm (Sui et al. 2015). Literature report suggests that 3D MoO_3-based semiconductor is very effective for various amine-based gas sensing (Malik et al. 2021). Due to excellent permeability involved to yolk-shell structure, the gas sensor based on yolk-shell nanoboxes of SnO_2/Au/Fe_2O_3 can detect a LoD of 50 ppb with a rapid response and recovery properties (Liu et al. 2019). ZIF-8-derived ZnO-$CsPbBr_3$ (Z-CPB) polyhedrons were found to be effectual in sensing TEA with response time of 2 seconds (Liu et al. 2022). The morphological features of Z-CPB are shown in Fig. 3.4a, b. The selectivity was very prominent for TEA for all the sensors as related to other analytes such as formaldehyde, ethanol, acetone, benzene, and acetonitrile as shown in Fig. 3.4c. In the mechanism, when $CsPbBr_3$ and ZnO come in contact, the free electrons from $CsPbBr_3$ transfer to ZnO until they reach equilibrium. Thus, at the interface, an electron depletion layer formed for $CsPbBr_3$ and an electron accumulation layer formed for ZnO. This interface between materials leads to the formation of an n-n heterojunction where more oxygen molecules can be adsorbed onto ZnO. The abundant electron resources on ZnO make it easier for this extra oxygen to be absorbed, improving gas-sensing performance (Fig. 3.4d). Spoiled meat product also releases gas like H_2S. Mesoporous hierarchical architectures of SnO_2 were fabricated using waste scallion root bio-template (Song et al. 2020). The working temperature of the gas detection system was set at 92 °C, which allowed for the successful detection of H_2S concentration with a limit of 0.5 ppb. This SnO_2-based sensor was effective in tracking H_2S concentrations during its decay process in fresh pork and human exhaled breath and within an environment containing high humidity levels.

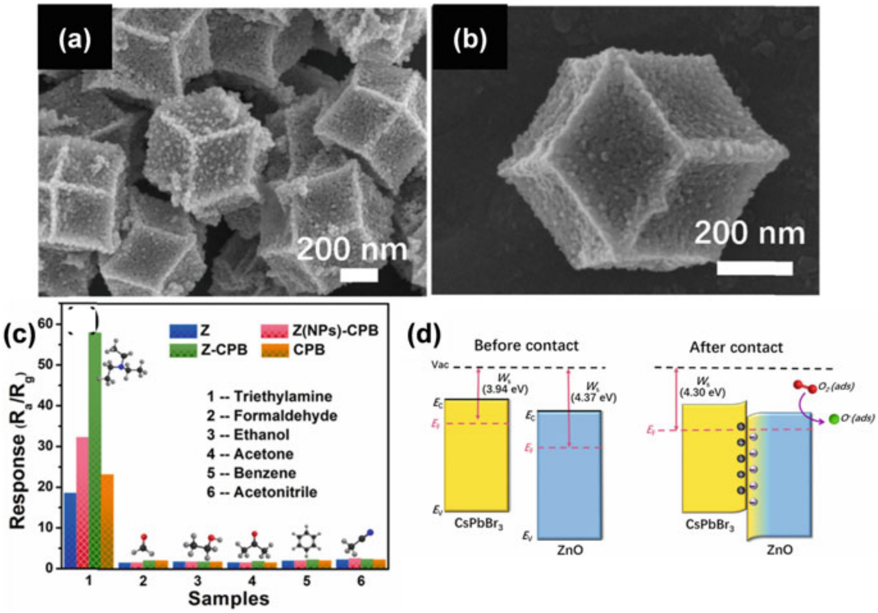

Fig. 3.4 (**a**, **b**) SEM images of Z-PCB, (**c**) selectivity of as-prepared sensors to different gases at 180 °C, and (**d**) energy-level diagram of Z-CPB. [Reprinted with permission from Ref. (Liu et al. 2022), copyright Elsevier]

Similarly, Cr_2O_3-based sensors were synthesized following the same bio-template method and successfully monitored the chicken freshness (Song et al. 2022).

From the reported literature, metal oxide-based gas sensors are far ahead of other sensing materials for various applications. However, 3D morphology-based gas sensors are not explored much as compared to 0D, 1D, and 2D materials. Further exploration on 3D nanostructure-based materials may result in better selectivity, sensitivity, response, and low working temperature.

3.4 Summary and Outlook

This chapter has summarized some topical 3D nanostructure-based materials for applications in gas sensing. Metal oxide-based semiconductors are found to be dominant in many sensing applications due to the ease in synthesis and fabrication, morphological tuning, good sensitivity, and faster response time. As most of the gas-sensing devices have higher operating temperature, the stability of MOSs-based materials in high temperature makes them suitable candidate for gas sensing. Besides pristine nanomaterials, heterojunctions, surface functionalization, doping, and composite materials also tailored the gas-sensing ability of many materials. It was found that the morphological and structural strategy such as exposed facet, porosity, hollow structure, and hierarchical structure can lead the way to a greater number of active sites and higher activity. In disease diagnosis, noninvasive exhaled breath gas sensors make them an ideal alternate to current standard methods. Still there are many critical issues which need to be improved further to get better selectivity, sensitivity, and response. Simultaneous detection of multiple gas analytes in a single device will be more beneficial. Long-term stability of these devices in ambient atmosphere is very poor which limits the applicability outside of lab environment. Materials with low operating temperatures will decrease the power consumption with a better stability, and this could be achieved by hybridization of metal oxides with various carbonaceous materials, chalcogenides, MXenes, metal nitrides, etc. Looking toward the future and with the recent global pandemic, innovations in this field will certainly lead to rapid, portable, and inexpensive diagnostics and accessibility all over the world.

References

Alam S, Ansari MS, Banik A, Ali R, Verma S, Qureshi M (2019) Ultrasensitive NOX detection in simulated exhaled air: enhanced sensing via alumina modification of in-situ grown WO_3 nanoblocks. Chem Asian J 14(24):4673–4680

Ansari MS, Banik A, Kalita A, Iyer PK, Qureshi M (2018) Multifunctional hierarchical 3-D ZnO superstructures directly grown over FTO glass substrates: enhanced photovoltaic and selective sensing applications. J Mater Chem A 6(32):15868–15887

Awano S, Ansai T, Takata Y, Soh I, Yoshida A, Hamasaki T et al (2008) Relationship between volatile sulfur compounds in mouth air and systemic disease. J Breath Res 2(1):017012

Bochenkov VE, Sergeev GB (2010) Sensitivity, selectivity, and stability of gas-sensitive metal-oxide nanostructures. In: Metal oxide nanostructures and their applications, vol 3. American Scientific Publishers, Stevenson Ranch, pp 31–52

Cao PJ, Li M, Rao CN, Han S, Xu WY, Fang M et al (2020) High sensitivity NO_2 gas sensor based on 3D WO_3 microflowers assembled by numerous nanoplates. J Nanosci Nanotechnol 20(3): 1790–1798

Chen X, Li JJ, Chen X, Cai SC, Yu EQ, Chen J, Jia H (2018) MOF-templated approach for hollow NiO_x/Co_3O_4 catalysts: enhanced light-driven thermocatalytic degradation of toluene. ACS Appl Nano Mater 1(6):2971–2981

Choi SJ, Jang BH, Lee SJ, Min BK, Rothschild A, Kim ID (2014) Selective detection of acetone and hydrogen sulfide for the diagnosis of diabetes and halitosis using SnO_2 nanofibers functionalized with reduced graphene oxide nanosheets. ACS Appl Mater Interfaces 6(4): 2588–2597

Das S, Pal M (2020) Non-invasive monitoring of human health by exhaled breath analysis: a comprehensive review. J Electrochem Soc 167(3):037562

Degler D, Weimar U, Barsan N (2019) Current understanding of the fundamental mechanisms of doped and loaded semiconducting metal-oxide-based gas sensing materials. ACS Sens 4(9): 2228–2249

Feng P, Wan Q, Wang TH (2005) Contact-controlled sensing properties of flowerlike ZnO nanostructures. Appl Phys Lett 87(21):213111

Firooz AA, Mahjoub AR, Khodadadi AA (2009) Highly sensitive CO and ethanol nanoflower-like SnO_2 sensor among various morphologies obtained by using single and mixed ionic surfactant templates. Sensors Actuators B Chem 141(1):89–96

Gouma PI, Kalyanasundaram K (2008) A selective nanosensing probe for nitric oxide. Appl Phys Lett 93(24):244102

Gurlo A, Bârsan N, Weimar U (2005) Gas sensors based on semiconducting metal oxides. In: Metal oxides. CRC Press, Boca Raton, pp 705–760

Huber F, Riegert S, Madel M, Thonke K (2017) H_2S sensing in the ppb regime with zinc oxide nanowires. Sensors Actuators B Chem 239:358–363

Isaac NA, Pikaar I, Biskos G (2022) Metal oxide semiconducting nanomaterials for air quality gas sensors: operating principles, performance, and synthesis techniques. Microchim Acta 189(5): 1–22

Jeong YJ, Koo WT, Jang JS, Kim DH, Kim MH, Kim ID (2018) Nanoscale PtO_2 catalysts-loaded SnO_2 multichannel nanofibers toward highly sensitive acetone sensor. ACS Appl Mater Interfaces 10(2):2016–2025

Jha S, Calvert JW, Duranski MR, Ramachandran A, Lefer DJ (2008) Hydrogen sulfide attenuates hepatic ischemia-reperfusion injury: role of antioxidant and antiapoptotic signaling. Am J Phys Heart Circ Phys 295(2):H801–H806

Kamoun P, Belardinelli MC, Chabli A, Lallouchi K, Chadefaux-Vekemans B (2003) Endogenous hydrogen sulfide overproduction in Down syndrome. Am J Med Genet 116(3):310–311

Kim HJ, Lee JH (2014) Highly sensitive and selective gas sensors using p-type oxide semiconductors: overview. Sensors Actuators B Chem 192:607–627

Konvalina G, Haick H (2014) Sensors for breath testing: from nanomaterials to comprehensive disease detection. Acc Chem Res 47(1):66–76

Koo WT, Yu S, Choi SJ, Jang JS, Cheong JY, Kim ID (2017) Nanoscale PdO catalyst functionalized Co_3O_4 hollow nanocages using MOF templates for selective detection of acetone molecules in exhaled breath. ACS Appl Mater Interfaces 9(9):8201–8210

Krishnakumar T, Jayaprakash R, Pinna N, Donato N, Bonavita A, Micali G, Neri G (2009) CO gas sensing of ZnO nanostructures synthesized by an assisted microwave wet chemical route. Sensors Actuators B Chem 143(1):198–204

Li Q, Li Z, Zhang Q, Zheng L, Yan W, Liang X et al (2021) Porous γ-Fe_2O_3 nanoparticle decorated with atomically dispersed platinum: study on atomic site structural change and gas sensor activity evolution. Nano Res 14(5):1435–1442

Lin C, Xian X, Qin X, Wang D, Tsow F, Forzani E, Tao N (2018) High performance colorimetric carbon monoxide sensor for continuous personal exposure monitoring. ACS Sens 3(2):327–333

Liu J, Peng Y, Zhu B, Li Y, Zhang L, Yu J (2022) ZIF-8 derived ZnO-$CsPbBr_3$ polyhedrons for efficient triethylamine detection. Sensors Actuators B Chem 357:131366

Liu L, Zhao Y, Song P, Yang Z, Wang Q (2019) ppb level triethylamine detection of yolk-shell SnO_2/Au/Fe_2O_3 nanoboxes at low-temperature. Appl Surf Sci 476:391–401

Ma J, Fan H, Zheng X, Wang H, Zhao N, Zhang M et al (2020) Facile metal-organic frameworks-templated fabrication of hollow indium oxide microstructures for chlorine detection at low temperature. J Hazard Mater 387:122017

Malik R, Joshi N, Tomer VK (2021) Advances in the designs and mechanisms of MoO_3 nanostructures for gas sensors: a holistic review. Mater Adv 2(13):4190–4227

Mane SM, Nimbalkar AR, Go JS, Patil NB, Dhasade SS, Thombare JV et al (2021) NO2 sensing properties of 3D flower-like ZnO nanostructure decorated with thin porous petals synthesized using a simple sol–gel drop-casting method. Appl Phys A 127(1):1–11

McCabe-Sellers BJ, Beattie SE (2004) Food safety: emerging trends in foodborne illness surveillance and prevention. J Am Diet Assoc 104(11):1708–1717

McGeer EG, McGeer PL (2010) Neuroinflammation in Alzheimer's disease and mild cognitive impairment: a field in its infancy. J Alzheimers Dis 19(1):355–361

Messenger J, Clark S, Massick S, Bechtel M (2013) A review of trimethylaminuria:(fish odor syndrome). J Clin Aesthet Dermatol 6(11):45

Mirzaei A, Leonardi SG, Neri G (2016) Detection of hazardous volatile organic compounds (VOCs) by metal oxide nanostructures-based gas sensors: a review. Ceram Int 42(14): 15119–15141

Narasimhan LR, Goodman W, Patel CKN (2001) Correlation of breath ammonia with blood urea nitrogen and creatinine during hemodialysis. Proc Natl Acad Sci 98(8):4617–4621

Neri G (2015) First fifty years of chemoresistive gas sensors. Chemosensors 3(1):1–20

Patil VL, Kumbhar SS, Vanalakar SA, Tarwal NL, Mali SS, Kim JH, Patil PS (2018) Gas sensing properties of 3D mesoporous nanostructured ZnO thin films. New J Chem 42(16):13573–13580

Peng G, Tisch U, Adams O, Hakim M, Shehada N, Broza YY et al (2009) Diagnosing lung cancer in exhaled breath using gold nanoparticles. Nat Nanotechnol 4(10):669–673

Periyasamy M, Kar A (2020) Modulating the properties of SnO_2 nanocrystals: morphological effects on structural, photoluminescence, photocatalytic, electrochemical and gas sensing properties. J Mater Chem C 8(14):4604–4635

Prajapati CS, Bhat N (2018, October) Growth optimization, morphological, electrical and sensing characterization of V_2O_5 films for SO_2 sensor chip. In 2018 IEEE Sensors (pp. 1–4). IEEE

Ren Y, Zou Y, Liu Y, Zhou X, Ma J, Zhao D et al (2020) Synthesis of orthogonally assembled 3D cross-stacked metal oxide semiconducting nanowires. Nat Mater 19(2):203–211

Rossinyol E, Prim A, Pellicer E, Arbiol J, Hernández-Ramírez F, Peiro F et al (2007) Synthesis and characterization of chromium-doped mesoporous tungsten oxide for gas sensing applications. Adv Funct Mater 17(11):1801–1806

Seinfeld JH, Pandis SN (1998) From air pollution to climate change. Atmospheric chemistry and physics, vol 1326. Wiley, Hoboken

Shi T, Hou H, Hussain S, Ge C, Alsaiari MA, Alkorbi AS et al (2022) Efficient detection of hazardous H2S gas using multifaceted Co_3O_4/ZnO hollow nanostructures. Chemosphere 287: 132178

Shin J, Choi SJ, Youn DY, Kim ID (2012) Exhaled VOCs sensing properties of WO3 nanofibers functionalized by Pt and IrO_2 nanoparticles for diagnosis of diabetes and halitosis. J Electroceram 29(2):106–116

da Silva LF, M'peko JC, Catto AC, Bernardini S, Mastelaro VR, Aguir K et al (2017) UV-enhanced ozone gas sensing response of ZnO-SnO_2 heterojunctions at room temperature. Sensors Actuators B Chem 240:573–579

Song BY, Zhang M, Teng Y, Zhang XF, Deng ZP, Huo LH, Gao S (2020) Highly selective ppb-level H_2S sensor for spendable detection of exhaled biomarker and pork freshness at low temperature: mesoporous SnO_2 hierarchical architectures derived from waste scallion root. Sensors Actuators B Chem 307:127662

Song BY, Zhang XF, Huang J, Cheng XL, Deng ZP, Xu YM et al (2022) Porous Cr_2O_3 architecture assembled by nano-sized cylinders/ellipsoids for enhanced sensing to trace H2S gas. ACS Appl Mater Interfaces 14:22302

Sui LL, Xu YM, Zhang XF, Cheng XL, Gao S, Zhao H et al (2015) Construction of three-dimensional flower-like α-MoO_3 with hierarchical structure for highly selective triethylamine sensor. Sensors Actuators B Chem 208:406–414

Wang C, Yin L, Zhang L, Xiang D, Gao R (2010) Metal oxide gas sensors: sensitivity and influencing factors. Sensors 10(3):2088–2106

Wang G, Yang S, Cao L, Jin P, Zeng X, Zhang X, Wei J (2021) Engineering mesoporous semiconducting metal oxides from metal-organic frameworks for gas sensing. Coord Chem Rev 445:214086

Wang Q, Yao N, An D, Li Y, Zou Y, Lian X, Tong X (2016) Enhanced gas sensing properties of hierarchical SnO_2 nanoflower assembled from nanorods via a one-pot template-free hydrothermal method. Ceram Int 42(14):15889–15896

Wang T, Can I, Zhang S, He J, Sun P, Liu F, Lu G (2018) Self-assembly template driven 3D inverse opal microspheres functionalized with catalyst nanoparticles enabling a highly efficient chemical sensing platform. ACS Appl Mater Interfaces 10(6):5835–5844

Willa C, Yuan J, Niederberger M, Koziej D (2015) When nanoparticles meet poly (ionic liquid) s: chemoresistive CO_2 sensing at room temperature. Adv Funct Mater 25(17):2537–2542

Wu X, Wang H, Wang J, Wang D, Shi L, Tian X, Sun J (2022) VOCs gas sensor based on MOFs derived porous Au@ Cr_2O_3-In_2O_3 nanorods for breath analysis. Colloids Surf A Physicochem Eng Asp 632:127752

Yang S, Sun J, Xu L, Zhou Q, Chen X, Zhu S et al (2020) Au@ ZnO functionalized three–dimensional macroporous WO_3: a application of selective H2S gas sensor for exhaled breath biomarker detection. Sensors Actuators B Chem 324:128725

Yoon JW, Lee JH (2017) Toward breath analysis on a chip for disease diagnosis using semiconductor-based chemiresistors: recent progress and future perspectives. Lab Chip 17(21):3537–3557

Yuan H, Aljneibi SAAA, Yuan J, Wang Y, Liu H, Fang J et al (2019) ZnO nanosheets abundant in oxygen vacancies derived from metal-organic frameworks for ppb-level gas sensing. Adv Mater 31(11):1807161

Yuliarto B, Gumilar G, Septiani NLW (2015) SnO_2 nanostructure as pollutant gas sensors: synthesis, sensing performances, and mechanism. Adv Mater Sci Eng 2015:1

Zhang C, Liu G, Geng X, Wu K, Debliquy M (2020) Metal oxide semiconductors with highly concentrated oxygen vacancies for gas sensing materials: a review. Sensors Actuators A Phys 309:112026

Zhao C, Gong H, Niu G, Wang F (2020) Ultrasensitive SO_2 sensor for sub-ppm detection using Cu-doped SnO_2 nanosheet arrays directly grown on chip. Sensors Actuators B Chem 324: 128745

Zhou Q, Xu L, Kan Z, Yang L, Chang Z, Dong B et al (2022) A multi-platform sensor for selective and sensitive H2S monitoring: three-dimensional macroporous ZnO encapsulated by MOFs with small Pt nanoparticles. J Hazard Mater 426:128075

Zhou T, Zhang T (2021) Recent progress of nanostructured sensing materials from 0D to 3D: overview of structure—property-application relationship for gas sensors. Small Methods 5(9): 2100515